Lecture 7

Crystal Growth: Engineering Solid/Melt Interface

In the previous lectures we have seen the crystallization from solutions, such as nucleation by evaporation or supercooling. These solution-based crystallization techniques are suitable for:

- Low melting point (T_m) materials (e.g. water $\rightarrow$ ice)
- Minor species dissolved in solvent (e.g. polymers, DNA, proteins)[1]

However such method is not suitable for high T_m and solvent-sensitive materials such as Si and sapphire. In semiconductor industry, the crystals are usually grown directly from the melt. There are several widely-used techniques for growing high quality single crystals of semiconductor, for example the floating zone (FZ) method.[2] A scheme of the FZ method is shown in Figure 7.1, where a quartz ampule of radius R containing crystal is slowly moved along the z-direction with speed v. A fixed radio-frequency (RF) heating coil is used to heat up a certain zone of the crystal. High purity crystal is obtained by moving the floating zone. We can model the floating zone in a cylindrical system. There are two zones with temperature T_1 and T_2, respectively, such that $T_1 < T_\mathrm{m} < T_2$. The ampule is moving at a constant speed v along the z-direction. We set $z = 0$ at the interface of the two temperature zones. Depending on the moving speed and thermodynamic properties of the system, the interface position z_m between the melt and crystal may vary (i.e. z_m can be either equal, lower or higher than 0). The system involves both heat and mass transfers, and we will solve them individually.

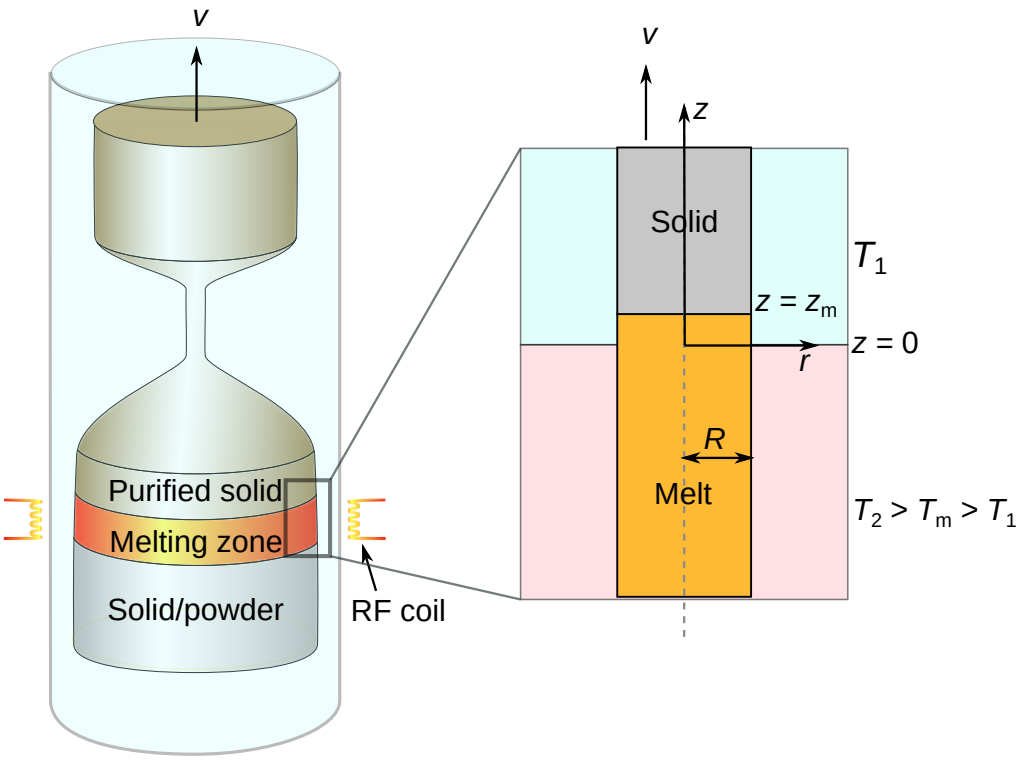

Figure 7.1: The floating zone method. Left: scheme of a typical floating zone setup. Right: zoom-in region near the interface between the melt and crystal. The position of the melt interface z_m may be different from the interface of heating zone ($z = 0$), due to the moving of the floating zone.

7.1 Heat transfer in floating zone

At steady state, both the crystal (S) and melt phases (L) move at the same speed v. Therefore the velocity of the interface $v_I = 0$. For the heat transfer problem we want to solve the distribution of T in both phases (T_S and T_L) as a function of r and z. The heat transfer equation in both phases is:

$$v\frac{\partial T}{\partial z} = \alpha\nabla^2 T = \alpha\left[\frac{1}{r}\frac{\partial}{\partial r}(r\frac{\partial T}{\partial r}) + \frac{\partial^2 T}{\partial z^2}\right] \tag{7.1}$$

where α is the thermal diffusivity of each phase (see Lecture 6). The boundary conditions are:

$$\begin{cases} \frac{\partial T}{\partial r} = 0 & r = 0 \\ -k\frac{\partial T}{\partial r} = h(T - T_1) & r = R; z > 0 \\ -k\frac{\partial T}{\partial r} = h(T - T_2) & r = R; z < 0 \end{cases} \tag{7.2}$$

where k is the thermal conductivity and h is the heat transfer coefficient.

Since we are more interested in the distribution of T along the z-direction, we can define an area-averaged temperature $\overline{T}$ for each z:

$$\overline{T}(z) = \frac{2\pi\int_0^R T\mathrm{d}r}{2\pi\int_0^R r\mathrm{d}r} = \frac{2}{R^2}\int_0^R Tr\mathrm{d}r \tag{7.3}$$

The new governing equation for $\overline{T}$ becomes:

$$\frac{\mathrm{d}^2\overline{T}}{\mathrm{d}z^2} - \frac{v}{\alpha}\frac{\mathrm{d}\overline{T}}{\mathrm{d}z} - \frac{2h(\overline{T} - T_\infty)}{kR} = 0 \tag{7.4}$$

where $T_\infty = T_1$ if $z > 0$, and $T_\infty = T_2$ if $z < 0$. The boundary conditions are:

$$\begin{cases} \overline{T}(z \to \infty) & = T_\infty = T_1 \\ \overline{T}(z \to -\infty) & = T_\infty = T_2 \end{cases} \tag{7.5}$$

Here we assume the variation of temperature profile in r-direction is smaller compared with z-direction, i.e. $T(R, z) \approx \overline{T}(z)$. Furthermore, at the crystal/melt interface ($z = z_m$) the temperature is $\overline{T} = T_m$, and heat balance condition gives:

$$-k_S\frac{\mathrm{d}\overline{T}}{\mathrm{d}z}|_S + k_L\frac{\mathrm{d}\overline{T}}{\mathrm{d}z}|_L = -\hat{\lambda}\rho(v - v_I) \tag{7.6}$$

where v_I is the velocity of the interface with respect to the heating zone, $\hat{\lambda}$ is the latent heat and ρ is the density (assuming $\rho_s = \rho_L = \rho$). The temperature profile along z can thus be solved by considering 3 cases ($z_m > 0$, $z_m < 0$ and $z_m = 0$) explicitly, by combining Equations 7.4 7.5 and 7.6. A typical profile of $\overline{T}(z)$ of the FZ is shown in Figure 7.2.

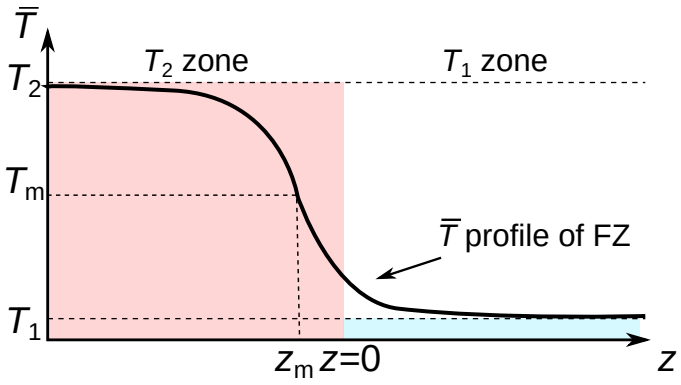

Figure 7.2: Profile of $\overline{T}(z)$ of the floating zone by solving the heat transfer equations. Color blocks indicate the position and temperature of the temperature zones.

7.2 Mass transfer in floating zone

Next we will solve the concentration distribution in the floating zone by using mass transfer at the interface. Here we assume that the interface moving rate $v_I \approx 0$. This is not exact since the interfacial temperature gradually decreases according to the phase diagram (Figure 7.3), but generally v_I is much slower than the zone moving speed v, and we can use the steady state $\overline{T}$ profile from the heat transfer analysis. Here we further assume the

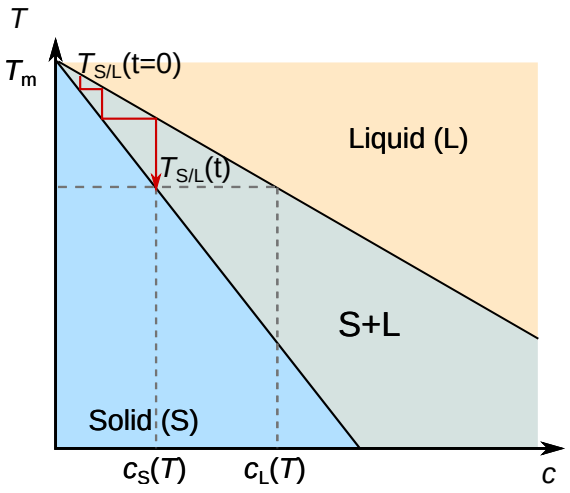

Figure 7.3: Change of interfacial temperature during the crystallization process (red path) seen from the binary phase diagram.

concentration of solute (impurity) is independent of r, which simplifies the mass transfer as a 1D problem. The concentration of solute is c_S, c_L and c_0 in purifies crystal, melt, and unpurified solid (polycrystal) regions, respectively. We define the length of the melt region as L. Depending on the region of interest, we can use different local coordinate systems.

Here x refers to the position when setting the purified crystal as rest frame, and y refers to the position when setting the crystal / melt interface as rest frame. Using this definition, c_S is expresses in $c_S(x)$ while c_L is expressed in $c_L(y)$, to avoid the issue with moving interface. The geometry of the floating zone setup and the definitions of the local coordinates can be seen in Figure 7.4.

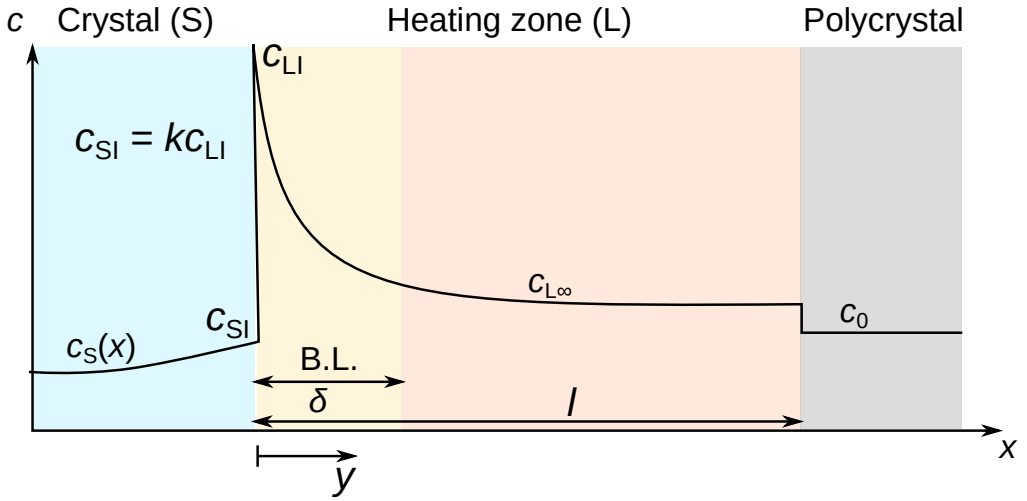

Figure 7.4: Concentration profile of the floating zone. Two coordinate systems x and y are used to describe the concentration in the purified solid and melt regions, respectively. A boundary layer with thickness δ is present at the melt interface.

At the solid-liquid interface, the interfacial concentration follows the partitioning rule (at constant T_m)[3] (see the phase diagram in Figure 7.3):

$$c_{SI} = kc_{LI} \tag{7.7}$$

where c_{SI} and c_{LI} are the interfacial concentrations in solid and liquid phases, respectively. c_{LI} is larger than the concentration far from the interface $c_{L\infty}$, since the impurities are injected from crystal to liquid. Therefore a boundary layer (B.L.) with thickness δ is present at the melt / crystal interface. To solve the concentration profile of $c_L(y)$, we employ the pseudo-steady state assumption that the diffusion time scale is much smaller than the interface moving time scale. The mass transfer equation in the liquid phase gives:

$$\mathcal{D}_L \frac{\partial^2 c_L}{\partial y^2} + v \frac{\partial c_L}{\partial y} = 0 \tag{7.8}$$

with boundary conditions:

$$\begin{cases} c_L(y=0) = c_{LI} \\ c_L(y=\infty) \approx c_L(y=\delta) = c_{L\infty} \end{cases} \tag{7.9}$$

The concentration profile $c_{\mathrm{L}}(y)$ has the solution:

$$c_{\mathrm{L}}(y) = \frac{c_0 - c_{\mathrm{LI}}(x)\exp(-\frac{\upsilon\delta}{\mathcal{D}_{\mathrm{L}}}) + [c_{\mathrm{LI}}(x) - c_0]\exp(-\frac{\upsilon y}{\mathcal{D}_{\mathrm{L}}})}{1 - \exp(\frac{\upsilon\delta}{\mathcal{D}_{\mathrm{L}}})} \tag{7.10}$$

where c_{LI} changes with the absolution position x of the interface. At the interface, the mass balance equation is:

$$\upsilon c_{\mathrm{LI}}(x) + \mathcal{D}_{\mathrm{L}}\frac{\partial c_{\mathrm{L}}}{\partial y}|_{y=0} - \upsilon\underbrace{c_{\mathrm{SI}}(x)}_{kc_{\mathrm{LI}}} - \mathcal{D}_{\mathrm{S}}\frac{\partial c_{\mathrm{S}}}{\partial y}|_{y=0} = 0 \tag{7.11}$$

where $\mathcal{D}_{\mathrm{S}}$ is the mass diffusion coefficient in the solid phase and can be neglected. Combine 7.11 and 7.10 we also get the solution for c_{SI}:

$$c_{\mathrm{SI}}(x) = c_{\mathrm{L}\infty}(x)\underbrace{\left[\frac{k}{k + (1+k)\exp(-\frac{-\upsilon\delta}{\mathcal{D}_{\mathrm{L}}})}\right]}_{k'} = c_{\mathrm{L}\infty}(x)k' \tag{7.12}$$

We can see that the concentration of the solid interface c_{SI} has a new partition coefficient k' with $c_{\mathrm{L}\infty}$. If the boundary layer δ is negligible compared with the length L, the concentration inside the floating zone can be regarded as uniformly $c_{\mathrm{L}\infty}$. Therefore by moving the FZ with a small amount $\mathrm{d}x$, $c_{\mathrm{L}\infty}$ increases by:

$$\begin{aligned} \mathrm{d}c_{\mathrm{L}\infty} &= \frac{(c_0 - c_{\mathrm{SI}})}{L}\mathrm{d}x \\ \frac{\mathrm{d}c_{\mathrm{SI}}}{c_0 - c_{\mathrm{SI}}} &= \frac{k'}{L}\mathrm{d}x \end{aligned} \tag{7.13}$$

which gives the solution of c_{SI} as function of x:

$$c_{\mathrm{SI}}(x) = c_0\left[1 - (1-k')\exp(-\frac{k'x}{L})\right] \tag{7.14}$$

Equation 7.14 is known as the Scheil equation.[4,5] Since the concentration in solid does not change, $c_{\mathrm{SI}}(x)$ is essentially $c_{\mathrm{S}}(x)$, which describes the concentration of the solute (impurity) in the crystal along x-direction. The Scheil equation indicates the concentration increases from $k'c_0$ (low impurity) at $x = 0$ to c_0 at $x \to \infty$ (high impurity). However in reality there is a region (impurity region) where the concentration becomes larger than c_0 that the Scheil equation cannot describe (Figure 7.5) The Scheil equation can be used to purify the semiconductor. In the region described by the Scheil equation the impurity concentration is smaller than the unpurified material c_0. By moving the heating coil several cycles we get the purified crystal on the left end of the solid phase.

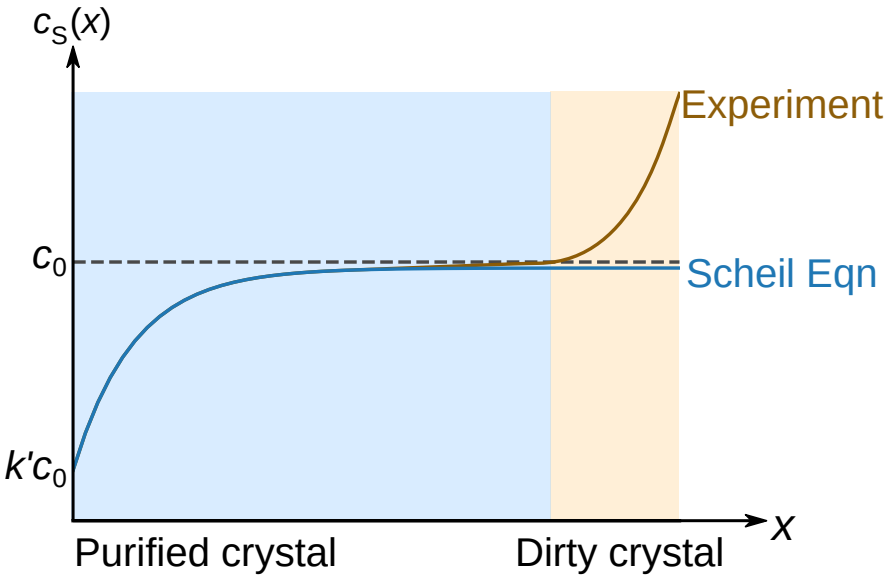

Figure 7.5: $c_S(x)$ profile from Scheil equation (blue) and from experiment (orange). The Scheil equation is in good agreement with experimental observations as small x while cannot capture the high impurity region near the crystal-melt interface.

References

(1) Franceschi, F. In *Protein Structure Analysis: Preparation, Characterization, and Microsequencing*, Kamp, R. M., Choli-Papadopoulou, T., Wittmann-Liebold, B., Eds.; Springer Lab Manual; Springer Berlin Heidelberg: Berlin, Heidelberg, 1997, pp 303–311.

(2) Keck, P. H.; Golay, M. J. E. *Phys. Rev.* **1953**, *89*, 1297–1297.

(3) Atkins, P.; Paula, J. d.; Keeler, J., *Atkins' Physical Chemistry*, Eleventh Edition; Oxford University Press: Oxford, New York, 2017.

(4) Gulliver, G. *J. Inst. Met* **1913**, *9*, 120–157.

(5) Scheil, E. *Z. Metallkd* **1942**, *34*, 70.